

# Detecting slope deformation using two-pass differential interferometry: Implications for landslide studies on Earth and other planetary bodies

M. H. Bulmer,<sup>1</sup> D. N. Petley,<sup>2</sup> W. Murphy,<sup>3</sup> and F. Mantovani<sup>4</sup>

Received 7 September 2005; revised 29 November 2005; accepted 16 February 2006; published 14 June 2006.

[1] Landslide features have been identified on Earth and the Moon, Mars, Venus, as well on the Jovian moons. By focusing on a terrestrial landslide complex we test the operational parameters of RADARSAT-1 and the use of two-pass differential interferometry to detect change, to map its extent, and to measure the amount of movement over a given time period. RADARSAT-1 was chosen because of its variable imaging modes and geometry. For investigations of landslide motions using remote sensing techniques, repeat-pass data are required. Synthetic aperture radar (SAR) interferometry (InSAR) can ideally monitor movements across the whole surface of a landslide to a millimetric precision, yielding a coverage significantly better than that obtained by ground instrumentation. Obtaining optimal data for InSAR analysis requires controlled orbital characteristics and imaging geometries, an understanding of the landslide characteristics and behavior, a cooperative surface, and mitigation of the factors that can affect phase. Using two-pass differential interferometry, a slope deformation map has been generated from RADARSAT-1 data for part of the Black Ven landslide ( $2^{\circ}52'W$ ,  $50^{\circ}40'N$ ), on the south coast of England. Four months separate the InSAR pair during which time 0.03 m of subsidence was measured. From this a movement rate of 0.09 m/yr can be calculated. This agrees well with ground observations and an in situ record of movement, thus demonstrating that the technique can be used to investigate landslides. With further refinement it can provide more direct measurements of landslide deformation on Earth and other planetary bodies than are currently available.

**Citation:** Bulmer, M. H., D. N. Petley, W. Murphy, and F. Mantovani (2006), Detecting slope deformation using two-pass differential interferometry: Implications for landslide studies on Earth and other planetary bodies, *J. Geophys. Res.*, *111*, E06S16, doi:10.1029/2005JE002593.

## 1. Introduction

[2] Landslides in coherent materials display a range of behavior styles, including long-term creep; creep that transitions into catastrophic failure; and catastrophic failure [Petley, 1996; Petley and Allison, 1997]. In all cases, rates of displacement are controlled by a range of variables that include pore pressure and total stress state, but the movement types primarily represent the style of deformation in the basal zone [Petley, 1996]. Within this zone, strain can accumulate through a range of processes including ductile deformation of a slice of material; through the nucleation and growth of new fractures or shear surfaces; or through sliding on one or more preexisting discontinuities [Petley *et al.*, 2002, 2005]. Terzaghi [1950] recognized that the

movement patterns of landslides provide an insight into the processes occurring in the basal deformation region, although care must be taken as surface displacements also reflect deformations occurring within the landslide mass itself.

[3] The investigation and interpretation of the patterns of movement associated with landslides have been undertaken using a wide range of techniques, including the use of in situ survey markers, extensometers, inclinometers, and remote techniques such as analog and digital photogrammetry, both terrestrial, airborne and spaceborne; and synthetic aperture radar interferometry (InSAR). However, in general these techniques suffer from serious shortcomings in terms of spatial and temporal resolution. Techniques such as extensometers and inclinometers are able to provide high-quality data over very small areas of the landslide, albeit with a potentially high temporal resolution. Although these data can be abundant they can be hard to interpret in terms of the evolution of movement across the whole landslide, especially in large and complex systems.

[4] For investigations using remote sensing techniques, repeat-pass data are required to extract information about landslide movement rates. The integration of SAR and TM

<sup>1</sup>Landslide Observatory, Joint Center for Earth Systems Technology, University of Maryland Baltimore County, Baltimore, Maryland, USA.

<sup>2</sup>International Landslide Centre, University of Durham, Durham, UK.

<sup>3</sup>School of Earth Sciences, University of Leeds, Leeds, UK.

<sup>4</sup>Dipartimento di Scienze della Terra, Università di Ferrara, Ferrara, Italy.

images, along with SAR interferometric techniques, are proving new ways characterize terrestrial landslides and supplement traditional air photo methods [Singhroy *et al.*, 1998]. SAR systems create a 2-D image in range and azimuth. One axis is in flight direction (along-track) and the other cross-track (slant-range), with the distance (phase) to the target measured by the time between pulse transmission and reception. Resolution in range (cross-track) depends on pulse width (shorter = better range resolution). An image in azimuth is created using the antenna “foot-print” on the ground (smaller = better resolution in azimuth). Signal processing in both range and azimuth directions is necessary to convert raw SAR data into an image. The image is distorted in the cross-track range direction.

[5] An interferometric image is the phase difference in two SAR images obtained from similar positions in space [Hanssen, 2001; Massonnet and Feigl, 1998]. Currently, spaceborne SAR systems have only one antenna so repeat pass data are acquired using two antenna positions from different orbits. Vertical height is determined by comparing phase measurements from the two images. Phase differences between images result from topography, changes in range due to displacement, or due to atmospheric effects. Local variations in atmospheric properties can cause differences in the path lengths between the two antenna positions and the target area. This can give rise to spurious phase variations which are superimposed onto the phase variations generated by the target area. Understanding factors that can affect phase is important when attempting InSAR analysis [e.g., Ferretti *et al.*, 2000]. Obtaining digital elevation maps from phase data requires that the SAR systems have well-maintained orbit paths and baseline separations. There are three main techniques used in differential InSAR studies [e.g., Massonnet *et al.*, 1993]: (1) four-pass, (2) three-pass, and (3) two-pass.

[6] In four-pass differential InSAR, two pairs of images are used. One InSAR pair supplies the external digital elevation model (DEM) while the other is used for differential processing. As the DEM does not have the same master as the pair that is used in the differential processing, there is a need to coregister the external DEM to the master.

[7] Three-pass differential InSAR requires three coherent InSAR images. Images 1 and 2 are used to make a DEM, and then 1 and 3 are used to produce an interferogram. The topographic phase estimated with image 1 and 2 is then subtracted to make a differential interferogram, showing change from image 2 to image 3. Advantages of this technique include (1) all images are projected into the space of image 1 and (2) it is not necessary to coregister an external DEM image to the master image. Additionally, the DEM obtained from the images is contemporaneous, and it will be densely sampled if there is good phase coherence.

[8] The two-pass technique is similar to the three-pass but with an additional step that requires fine-coregistration of the external DEM in true slant range coordinates to the master SAR image.

[9] While data from ERS and JERS have mainly been used in studies of landslides [Carnec *et al.*, 1996; Squarizoni *et al.*, 2003] this study tests and validates the extent to which the derived vertical change product from two-pass differential analysis of RADARSAT-1 data can measure the

development of strain in landslides. RADARSAT-1 has advantages over other SAR sensor in its viewing geometry and resolution making it potentially more suitable to landslide studies. However, it was not designed for InSAR studies, which only became possible once the orbital parameters were refined in 2001. RADARSAT-1 is C band and one fringe is equal to 2.8 cm. The strengths and limitations of the two-pass technique are established by comparing a derived deformation map obtained at the Black Ven landslide complex, on the south coast of England, with ground observations and motions measured by in situ instruments.

[10] Our goal is to better understand landslide processes on Earth as well on other bodies in the solar system. To this end, we have focused on Black Ven and have attempted to capture lessons about orbital geometries, SAR instrument capabilities and factors that can affect phase that can be relevant to future instrument design and mission planning to Mars and Venus. By focusing first on a terrestrial example, we have determined working parameters necessary for an orbital SAR system to obtain suitable data for InSAR analysis of landslides. Additionally, we have verified that the two-pass technique can be used to detect subsidence. If a SAR mission were to be planned for Mars or Venus we believe that differential InSAR analysis could be used to determine whether landslide deformation is ongoing, and at what rate.

## 2. Field Site

[11] The Black Ven landslide complex ( $2^{\circ} 52' W$ ,  $50^{\circ}40' N$ ) is situated in a temperate climate on the south coast of England between Charmouth and Lyme Regis in the county of Dorset (Figure 1). The landslide is  $\sim 2$  km wide and  $\sim 1$  km long, with a significant rotational component in the upper reaches, and an active mudflow component that is about 750 m long and 300 m wide [Brunsden and Jones, 1972; Brunsden *et al.*, 1975]. The calculated long-term mean retreat rate of the cliffs is 0.71 m/yr [Bray *et al.*, 1991]. The geological succession is relatively simple. The lowest part of the landslide is composed of interbedded mudstones, limestones and shales of lower Jurassic age. The bedding is gently inclined ( $2-3^{\circ}$ ) toward the southeast. The lower Jurassic succession seen at Black Ven is composed of the Blue Lias, Shales with Beef, Black Ven Marls and the Belemnite Marls formations. The top of the lower Jurassic sequence is marked by an unconformity, on top of which are situated the Cretaceous rocks of the Gault Clay and Upper Greensand (Foxmould) formations. Landslide activity is triggered through the build up of water within the permeable strata above the impermeable Jurassic mudstones.

[12] The morphology of the site is dominated by the geologic conditions. Rotational failures of Upper Greensand blocks in the headscarp allow the build up of slope debris. During the winter this debris becomes saturated, initiating ‘sand runs’ over the lower benches. This induces undrained loading of the lower portions of the landslide, inducing periodic rapid surges of material that extend over several hundreds of meters [Denness *et al.*, 1975]. Movement primarily occurs in March-April, when the winter and spring rainfall has had time to permeate to depth, although Moore and Brunsden [1996] controversially proposed that

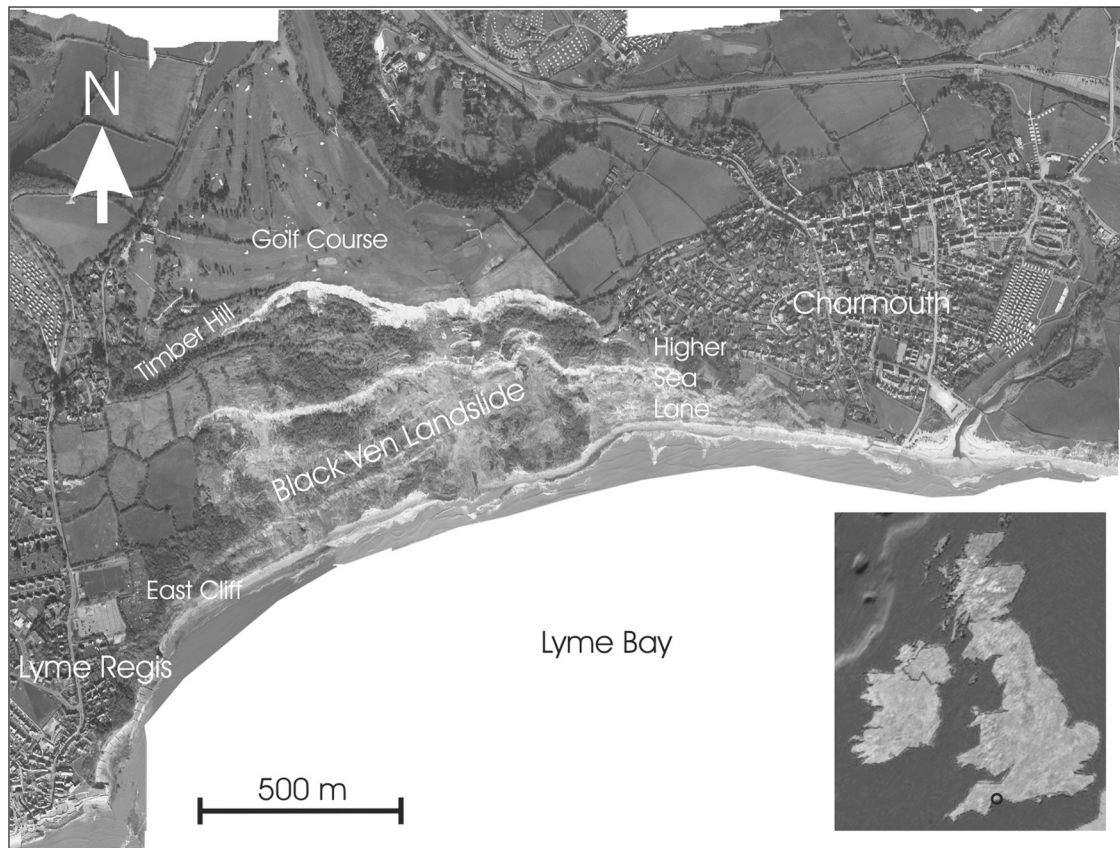


**Figure 1.** Air photo mosaic of the Black Ven landslide complex situated between Lyme Regis and Charmouth to the west and east, respectively.

there may be a pore fluid chemistry effect as well. The soils that form the sliding mass have a low cohesion ( $c' = 10\text{--}14$  kPa) and a moderate frictional strength ( $\phi' = 20\text{--}24^\circ$ ), with liquid limits of 71–72%, plastic limits of 30–33% and a plasticity index of 38–41%. The dominant clay minerals are kaolinite, illite and montmorillonite.

[13] During the winter of 1957/1958, a series of extensive failures occurred, resulting in two lobes of material extending 122 m into the sea [Brunsden and Jones, 1972]. Additionally, two big movements occurred on 7 August 1994, and creep has continued on the East-Cliff part of the landslide complex. In the winter of 1999, there was movement on the west flank and the rear scarp extended laterally. Repeated movements on this flank have caused damage to communications networks and buildings in the town of Lyme Regis.

[14] During the early 1970s the Institute of Geological Sciences conducted a study to explain the mechanisms behind the landslide movement [Conway, 1974]. Most recently, West Dorset District Council (WDDC), with its principal consultants High-Point Rendel, have carried out a series of interdisciplinary studies to gain an understanding of the coastal system from the subtidal zone to the top of the coastal slope. Aerial photogrammetric [Chandler and Brunsden, 1995; Brunsden and Chandler, 1996; Murphy and Inkpen, 1996] and LiDAR [Adams, 2001] surveys of the landslides, geomorphologic mapping, analysis of the nature, distribution and timing of landslide events, analysis of historical rainfall data, cored boreholes, trial pitting,

exposure logging, and geotechnical laboratory testing have all been conducted. In addition, there has been monitoring of ground movements using inclinometers, slip indicators, a Global Positioning System (GPS) survey, and visual observations [Fort *et al.*, 2000]. Monitoring of groundwater pressures has been achieved using manual and automated piezometers.

[15] The instrument record suggests that the landslide complex can be divided into three regions: East Cliff, Black Ven, and Higher Sea Lane (Figure 1). At present the monitoring record is most comprehensive at East Cliff, where the landslide affects the town of Lyme Regis, and thus is monitored by WDDC. Even with this extensive knowledge, monitoring and forecasting the behavior of this landslide complex remains problematic.

### 3. SAR Analysis

[16] The Black Ven complex represents a challenge for differential InSAR techniques. The slope angles at the landslide complex range from  $<10^\circ$  on the sand and mudflows to  $>60^\circ$  on the cliffs. Thus, to reduce image layover, foreshortening and distortion, incidence angles greater than  $35^\circ$  are required which can be attained by RADARSAT-1 in standard ( $20\text{--}49^\circ$ ) and fine ( $35\text{--}49^\circ$ ) beam modes [Singhroy and Saint-Jean, 1999; Singhroy and Molch, 2004].

[17] InSAR measures displacements only in slant-range and can only map motion at characteristic temporal and spatial scales related to the spatial resolution of the sensor

and the repeat-pass time [Singhroy *et al.*, 2003]. The landslide movements on Black Ven have a dominantly north-south orientation. Since this is approximately the orbital track of RADARSAT-1, displacements are in the across-track (range) direction. The movement rates on the landslide complex vary from mm/week to m/day. However, over the complex as a whole there is a characteristic pattern of creep, and increasing rates of movement that could represent the later stages of progressive failure. Movements on the order of <10s mm/month are suitable for detection in 24 day repeat-pass of RADARSAT-1. Faster movement rates occurring at Black Ven exceed the phase gradient limit [Carnec *et al.*, 1996], which eliminate interferometric correlation [Vachon *et al.*, 1995; Massonnet and Feigl, 1998] and could only be studied during occasional special orbital configurations with shorter repeat periods, such as those of ERS-1-2. The detection of slope deformation using differential InSAR is therefore dependent upon the style of deformation, the repeat period of the SAR sensor and its geometry relative to the direction of movement of the landslides. Additional factors that can affect SAR data over Black Ven include atmospheric effects, high rainfall during the winter months and rapid vegetation growth in the spring.

[18] Beginning in February 2001 the orbital position of RADARSAT-1 was maintained within  $\pm 2$  km of the nominal tracking, making InSAR analysis possible. With improved control over its orbital path and therefore baseline accuracies, RADARSAT-1 data offers greater flexibility in resolution and incidence angle than ERS-1-2 for InSAR studies. Archived RADARSAT-1 images for Black Ven acquired after February 2001 were referenced to known periods of movement on the ground as recorded by WWDC instrumentation. Additional geologic factors considered in image selection included the aerial extent of any movement and its orientation relative to the beam mode resolution and satellite orbit; local and regional slopes; vegetation; land use; soil moisture; and weather conditions. Following this initial image selection, the horizontal and perpendicular baseline separations were examined [Singhroy, 2004]. After consideration of these factors, useable InSAR pairs over Black Ven were found to be limited to only a few opportunities. A request for RADARSAT-1 data scheduling and programming was placed with the Alaskan SAR Facility (ASF). The first data opportunity was Standard Beam 5, at 30 m resolution with the incidence angle being  $36\text{--}42^\circ$  acquired in March 2001, with a second image to be collected 24 days later. In total, eight pairs were acquired between March 2001 and March 2002. Signal data (Level 0) were processed using Atlantis APP for SAR software and single look complex (SLC) images were created. These were taken into Earthview InSAR Software for InSAR analysis.

[19] Examination of the baselines of the InSAR images suggested that the data were best suited for two-pass differential analysis. The pair with the most suitable baseline separation (shortest distance between the two satellite orbits) and spectral overlap in range and azimuth were obtained in descending orbit on 4 November 2001 and 4 March 2002. The former was used as the "master" and the latter as the "slave." The perpendicular and parallel baseline separations of the images are 172 m and 117 m respectively. The spectral overlap in azimuth of master onto

slave is 85% and the range spectral overlap is 90%. The two SAR images were processed to produce a differential interferogram using an external DEM.

[20] This external DEM was derived from LiDAR data acquired in May 2001. The aim of using the external DEM for mapping landslide displacement was to remove topographic information from the differential interferogram. The remaining phase should then be the displacement between the two SAR images. All data were reprojected to Latitude and Longitude with a WGS84 datum. Manual coregistration of an external DEM to the Master was performed using 20 tie points after the DEM had been projected from latitude and longitude to true slant range/azimuth coordinates. The tie points were marked between the master SAR image and the simulated SAR image. The quality of each tie point was evaluated to a two-dimensional mapping polynomial function. Baseline estimates derived from the external DEM heights were used for residual phase removal. The total topographic phase, which includes the flat Earth phase and the topographic phase, was compared to a model for the total interferometric phase. This model was derived from the SAR acquisition geometry, the external DEM height, and the baseline.

[21] In the enhanced interferogram most of the topographic phase was subtracted, rendering the residual flat earth phase visible. Inspection of the enhanced interferogram phase showed fringes covering 1 to 1.5 cycles, indicating that the flat earth phase had not been completely removed during interferogram generation. Residual flat earth phase was expected because of inaccuracies in the reported RADARSAT-1 orbital information and deviations of the characteristics of the Black Ven site from the flat earth model. Some residual topographic information exists since the residual phase fringes are not straight and parallel. Residual topographic phase occurs because of a lack of precision in the coregistration of the master image with the DEM and uncertainties in the baseline geometry.

[22] To correct for residual phase the relationship between the master and the slave SAR images was optimized by altering the slave orbit using a baseline correction. The new geometry was then used to recalculate and remove the residual flat earth phase. The best correction for flat earth phase was made by reducing the perpendicular baseline by 19 m, to 153 m (Figure 2). Adjusting the perpendicular baseline value causes the vertical flat earth phase fringe spacing or slant range phase slope to change. The yaw angle was not altered. Residual topographic phase was removed using the same technique as for residual phase. The best correction for topographic phase was made by reducing the perpendicular baseline by 20 m, to 152 m (Figure 2).

[23] The interferogram phase was unwrapped using an Iterative Disk Masking algorithm from Atlantis Scientific. The calculated coherence image shows areas of high coherence over Lyme Regis and Charmouth but poor coherence over the landslide mass (Figure 3a). An iterative approach in which the coherence threshold was set allowed for additional unwrapping. The starting threshold was set high (0.05) to mask all low coherence values and gradually reduced by increments of 0.1 to a final value of 0.01. Areas around Lyme Regis and Charmouth were unwrapped (Figure 3b). However, over much of the landslide the coherence was too low to allow for unwrapping. No small

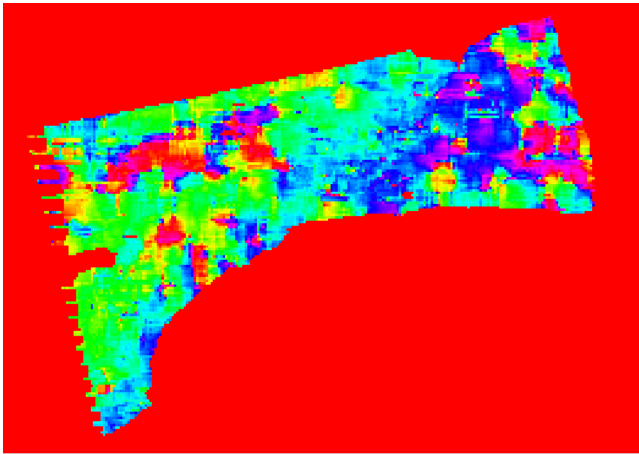


**Figure 2.** An enhanced interferogram after residual flat earth phase and topographic phase removal using a baseline correction method.

buildings and rock outcrops within the vegetated areas of the landslide could be identified to provide stable and accurate measurements (stable scatterers), to increase the useful area of the interferogram [Ferretti *et al.*, 2000, 2001].

#### 4. Results of Change Detection

[24] In differential mode, a DEM was generated from phase. Surface deformation was expressed as two products, vertical and horizontal change either as upsidence or subsidence. In the vertical change map upsidence is motion toward the sensor along the vertical direction and subsidence motion away in the same direction. In the horizontal change map, positive motion is way from the sensor and negative toward it. The terrain corrected image was reprojected to UTM and overlain on a shaded relief derived from the same LiDAR data that was used to make the external DEM for the 2 phase analysis. The vertical change image was the most useful and shows subsidence on the western side of the Black Ven landslide complex at East Cliff and in Lyme Regis (Figure 4). The amount of subsidence ranges from 0.02 m to 0.03 m over a period of 120 days. By multiplying these values by 3 an annual rate of movement of 0.06 to 0.09 m/yr can be calculated. To the east of Charmouth is the Stonebarrow landslide complex on which vertical change (0.03 m over 120 days) is seen below the backscarp. Here the basal Liassic strata is capped by poorly consolidated Lower Cretaceous sediments. Landslides are common with the mechanism for failure being similar to that of Black Ven. The mean rate of cliff retreat has been estimated to be between 0.2 and 0.4 m/yr [Bray *et al.*, 1991]. The calculated rate of 0.09 m/yr from the InSAR analysis is reasonable. Subsidence at East Cliff and within Lyme Regis will be discussed in greater detail in the next section.

#### 5. Comparing the Change Map to Ground Measurements and Observations

[25] On the basis of the InSAR generated change map (Figure 5), subsidence has occurred on the west side of

Black Ven between Lyme Regis and Charmouth. An active area of the landslide complex can be seen between the third and fourth benches to the east of East Cliff. The shape of the area of subsidence is arcuate and indicates that material is moving from the upper bench and spreading down slope. The recorded rate is between 0.02 to 0.023 m over 120 days from which a rate of movement of  $\sim 0.06$  m/yr is calculated. This is not a part of the landslide that is instrumented but the InSAR result is consistent with slow moving mudslides that were mapped from air photos acquired on 16 February 2002 (Figure 6).

[26] The area of East Cliff has historically been active and hence is periodically monitored by WDDC. Of particular interest is the area of the Fort Davey Football Ground southward to the sea cliff (Figure 5). The northern bank of the Ground and the touchline were reported to be moving from 1996–1998 and again over the winter of 2000/2001. The bank on the south side of the Ground showed slippage from 1996–1998 and again over the winter of 2000/2001. Surface deformation is particularly noticeable in the Charmouth Road Car Park where bulging of the tarmac surface occurs and painted lines have become distorted. Below the car park, a series of terraces are being formed by small

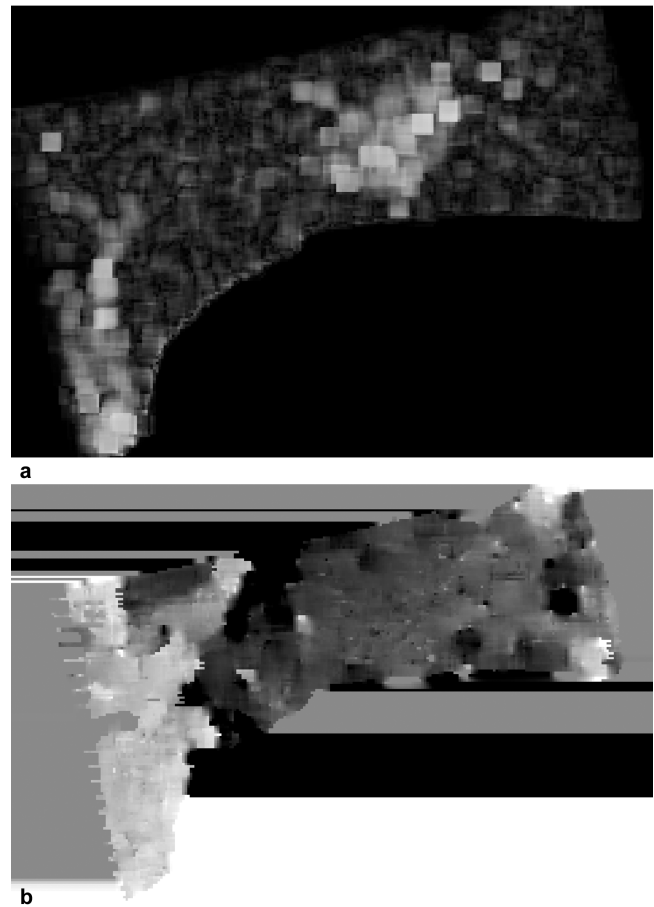


**Figure 3.** (a) A coherence image showing the highest values over Lyme Regis and Charmouth. (b) An unwrapped phase image. Note that Lyme Regis was successfully unwrapped. However, large parts of Black Ven could not be successfully unwrapped.

**Subsidence**  
Meters

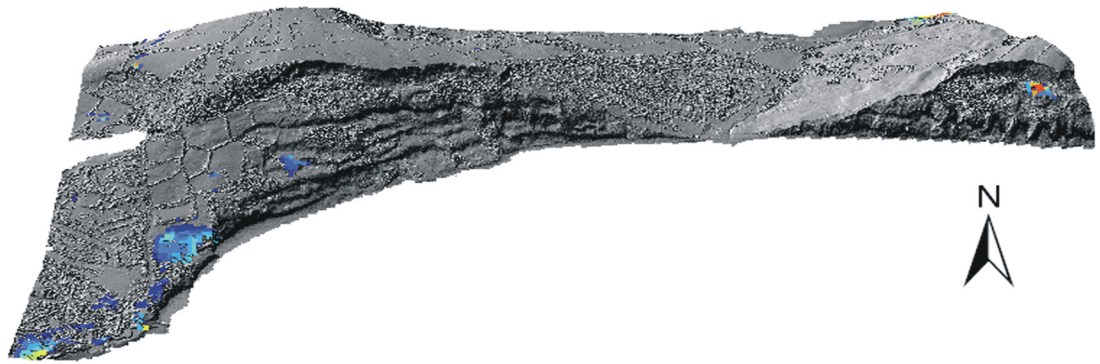
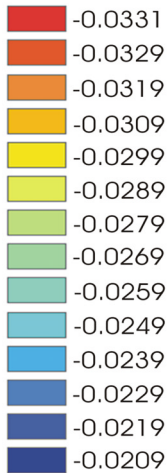


**Figure 4.** A color-defined vertical change map derived from the DEM generated from phase overlain on a hillshade extending from Lyme Regis to Stonebarrow. The colors in the top left and right are errors in the change map generation.

rotational movements. The backscarp was ~20 m below the car park in February 2001. There was large-scale movement associated with heavy rains in September 2000. Between January and April 2000, a spur of ground between East Cliff and the allotment system immediately to the east became disrupted, with several large blocks breaking away, and the cliff top retreated by several meters. The increased movement ruptured a drainage pipe buried in the slope.

[27] Figure 5 shows that the InSAR map of the area of subsidence around the Charmouth Road Car Park is arcuate in shape and is in good agreement on the margins with the mapped boundaries of landslide systems for East Cliff [Brunsden, 2002, Figure 46]. Interestingly, the area of subsidence on the map extends back into the car park to the edge of the Fort Davey Football Ground. The overall shape of the area of subsidence shows a headward movement that is NW in orientation. This cuts across the toe area

of a larger landslide proposed by *Brunsden* [2002] that is orientated north/south and extends back to Timber Hill. The amount of subsidence measured from the InSAR analysis of 0.02 m to 0.025 m over 120 days produces a rate of movement of 0.06–0.065 m/yr. This rate can be compared with movement rates recorded by instrument B207 on the southern edge of the Charmouth Road Car Park [Brunsden, 2002, Figure 45]. Over the period from February 1997 to February 2001 112 mm of movement was recorded at B207 giving an annual rate of 0.028 m/yr. These movement rates indicate slow creep in the Upper Greensand related to wetting of the slopes over the winter. During January and February 2002, 237 mm of rain fell which may account for the movements over the InSAR pair.

[28] In addition to East Cliff, displacement is shown in Figure 5 as occurring immediately to the west of Cobb Gate centered on the area of Longmoor and Lister Gardens. This

**Subsidence**  
Meters

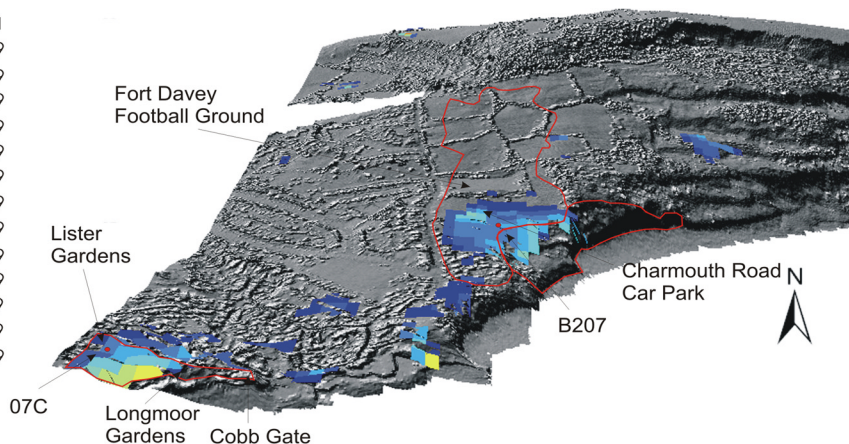
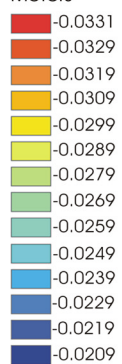


**Figure 5.** Subsidence at East Cliff and along Cobb Road from the InSAR analysis overlain on a shaded relief with landslide boundaries and movement vectors shown from *Brunsden* [2002].

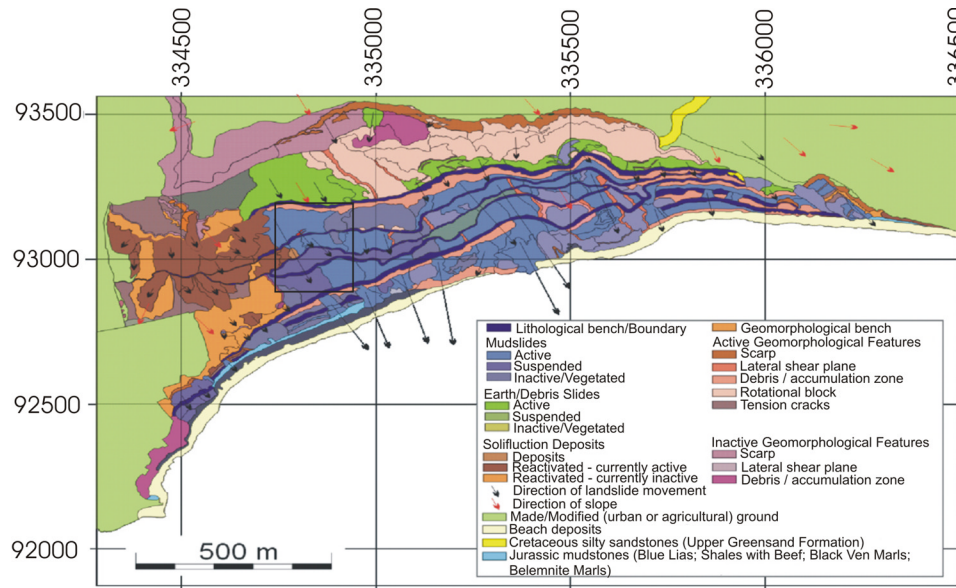


**Figure 6.** A geomorphic map showing landslide material and the interpreted sense of motion based on air photo analysis of images acquired 16 February 2002.

is a separate landslide complex to Black Ven and has a relatively dense array of inclinometers that have recorded movement seaward in a southeasterly direction. Ground cracks in the area were reported to have widened over 2000/2001. Figure 5 shows an area of subsidence that is arcuate and in good agreement with mapped outlines of landslide systems and ground behavior [Brunsden, 2002, Figure 45]. The orientation of the headward movement is to the northwest, which is also in line with assessments based on ground observations. The largest amount of subsidence (0.028 m over 120 days) is closest to the sea with the slower rates (0.02 m over 120 days) upslope in the backscarp region. This indicates more movement at the toe than is observed at the East Cliff site. Using these values from the InSAR a movement rate between 0.06 to 0.09 m/yr can be calculated. This can be compared to movement readings at instrument 07C [Brunsden, 2002, Figure 33]. Over the period from February 1997 to 2001, 156 mm of movement was recorded giving an annual rate of 0.039 mm/yr. The annual rates of movement between the InSAR study and from 07C are in broad agreement and are indicative of slow creep. The higher annual rates from the InSAR over the winter of 2001/2002 are likely a response to the relatively high winter rainfall.

## 6. Discussion

[29] There are two main inferences that can be drawn from our analysis. The first relates to detecting landslide displacements at Black Ven and the second to improving future InSAR analysis of landslide displacements. With reference to the first, Figures 4 and 5 show that vertical displacements can be obtained from two-pass differential analysis of RADARSAT-1 data. Vertical change maps can be used to detect movement, to determine the area that is affected, and the amount relative to a given time interval. This can then be used to calculate a rate of movement. RADARSAT-1 offers greater flexibility in resolution and

incidence angle over ERS-1/2 and JERS-1 data [Ferretti *et al.*, 2005] though is limited to a 24-day repeat period thereby restricting its application to slow moving landslides (<10s mm/month). A clear understanding is required of regions within any area of interest whose phase could not be unwrapped because of a lack of coherence. The lack of coherence may be due to either uncooperative ground conditions, displacements, or atmospheric effects. In the absence of any objects on the landslide that have a stable, point-like behavior [Ferretti *et al.*, 2005], improved coherence for two-pass differential could be achieved by positioning corner reflectors on the landslide complex. Alternatively, Raucoles *et al.* [2004] demonstrated that if an L-band SAR were available it could be used to overcome the loss of coherence observed in C-band. Given the 120 day period between the InSAR pair used in this analysis, any mapped displacements and derived calculations of movement rate must wherever possible be compared to observations and measurements made in situ on the ground. The displacement values are the total rate for the 120 days and do not allow for any periodicity within that time period to be distinguished.

[30] In addition to the ability to detect displacements, the second inference from our analysis is that the likelihood of detecting landslide displacements can be increased if careful consideration is given to SAR orbital and imaging geometries in relation to the landslides to be studied. A precisely maintained orbit or flight path is required to obtain useable InSAR pairs. To effectively image landslide details the SAR should have high-resolution (<5 m) and be able to image at variable incidence angles to reduce shadowing and layover. The wavelength of the SAR can also affect the coherence as well as the backscatter coefficient. Landslide deposits made up of rocks larger than the wavelength can cause them to appear smooth in the backscatter coefficient [Bulmer *et al.*, 2001]. Repeat-pass periods need to be responsive to the likely rates of movement on the ground. Fast moving landslides can only be studied using a SAR with two

antennas or by having more than one system flying in formation such as ERS 1 and 2. It is clear from the analysis of RADARSAT-1 data of Black Ven that InSAR can become a valuable tool in studying and monitoring landslides.

## 7. Conclusions and Implications for InSAR Studies on the Terrestrial Planets

[31] Using a two-pass differential technique landslide deformation has been detected and a map showing the areas affected compiled. Additionally, displacement rates over the 120 day interval between the RADARSAT-1 pairs can be used to calculate a rate of movement. This provides a methodology for improved remote geologic interpretation of landslide behavior and allows for the identification of slope movements. The area of a landslide that can be unwrapped is dependent upon the level of phase coherence. If this is high then the technique allows for larger areas to be examined than are currently possible with existing ground instrumentation, which is both spatially and cost constrained. Improved understanding of a landslides behavior requires both the area affected and the rates of subsidence within discrete zones to be identified and calculated. For example, at East Cliff, the movement above the seawall shows low rates of displacement, with the backscarp extending back into the Charmouth Road Car Park. This is also the case at Longmoor Gardens. The rates of movement over the 120 days between the two SAR images from which an annual rate (0.06 to 0.09 m/yr) can be calculated are characteristic of creep. This is likely related to increased wetting of the ground by the winter rains. Ground instruments that record movement over a defined time period can provide an essential calibration of the InSAR results without which the rates of movement cannot be validated. This poses a possible problem for InSAR studies of landslides on Mars and Venus but can be overcome by comparing any displacement rates with those recorded on landslides on Earth, such as at Black Ven, where detailed geomorphic and instrumented data exist.

[32] Landslides have been identified on the Moon, Mars, Venus, and on the moons of Jupiter but high-resolution images and topography remain limited and measurements of displacement rates have not been possible. In the next section, the ability to acquire SAR data on Mars and Venus for InSAR analysis is discussed in greater detail.

### 7.1. Mars

[33] Mars Global Surveyor (MGS) Mars Orbiter Camera (MOC) and Mars Laser Altimeter (MOLA) data have revealed new details of landslides [e.g., *Malin et al.*, 1998; *Smith et al.*, 1998] but do not allow for quantitative determination of movement. There are many interpretations of Martian landslide origin, behavior style, and emplacement. Landslides in the Valles Marineris have been interpreted to be the result of large-scale catastrophic failures capable of producing long runout landslides [*Luchitta*, 1978, 1979, 1987; *McEwen*, 1989; *Shaller*, 1991]. As an alternative, *Bulmer and Zimmerman* [2005] have suggested that landslide morphologies at Ganges Chasma might be explained by gravity driven creep on the >2 km high canyon walls that has occurred over long periods of time. Long-

duration gravity-driven movements can also explain the morphologies and dimensions of small volume talus lobes. The movement of lobes is suggested to be analogous to periglacial rock glaciers.

[34] Earth-based radar imaging of Mars indicates that substantial penetration of the surface (meters) is obtained at 12 cm radar wavelength [*Elachi et al.*, 1984]. Recent laboratory measurements of terrestrial analogs for Martian soils and rocks, combined to numerical modeling, indicate that a P-Band (70 cm) SAR should penetrate at least 5 m deep [*Paillou et al.*, 2001]. Shuttle radar observations of terrestrial deserts revealed subsurface structures to depths of about 2 m using L-Band (24 cm) radar [*Elachi et al.*, 1984]. Building on these lessons an orbital SAR for Mars exploration (The Mars Environment Evolution Mission MEEM) has been proposed that would use a dual-frequency SAR (L and P-Bands) to map the planet at 50 m resolution, penetrating 5–10 m over much of the surface [*Team X*, 2000]. Selected targets will be imaged at 5 m resolution. Using repeat-pass interferometry, a 50 m resolution topographic map will be acquired within a year, and surface changes will be detected and monitored for two additional years. The mission would launch in August or September 2009, followed by an Earth to Mars cruise with an arrival at Mars in July or August 2010 followed by circularization of its orbit. Data acquisition would commence in July 2011 and continue for a year until July 2012.

[35] On the basis of our observations of landslides on Mars, this mission has the potential to detect displacements over a range of styles of landslides. The repeat-pass cycle is not currently known but we advocate a range from 7 to 28 days and variable incidence angles from 20° to 50°. The generation of a DEM using Mars Express High-Resolution Stereo Camera (HRSC) data at 10–2 m resolution will allow an external DEM to be used in InSAR analysis of MEEM data.

### 7.2. Venus

[36] The Magellan Radar Mission to Venus which used an S-band (12.6 cm) SAR, confirmed evidence for slope failures at a variety of scales [*Saunders et al.*, 1992; *Malin*, 1992]. Raw SAR data were processed into image strips [*Ford et al.*, 1989; *Saunders et al.*, 1992]. Many volcanic domes appear to have had their circular planforms altered by rotational and translational slope failures [*Bulmer and Guest*, 1996; *Bulmer and Wilson*, 1999], some of which produced runout distances of tens of kilometers [*Bulmer and Guest*, 1996; *Bulmer*, 1994]. In addition to the failures on the flanks of domes, a range of mass movement morphologies exists in highland regions and escarpments [*Malin*, 1992; *Bulmer*, 1997].

[37] Magellan repeated its coverage of Venus every 240 days, and there were three cycles, so the potential existed to observe a landslide. However, complicating factors were the elliptical orbit of the spacecraft and the constantly changing altitude with latitude [*Johnson and Edgerton*, 1985]. The orbit ellipticity, imaging geometry of repeat passes and mode of operation of Magellan also negated comparison of phase difference between two images. However, *Lee and Morgan* [2002] have used the hundreds of pulses contained in one burst to generate two subaperture complex images with different center pulse time offsets and coherent inte-

gration times. A vector between two center pulse positions forms a baseline vector. Range and azimuth compression and coregistration of the two subaperture complex images result in an interferometric signal in the range Doppler domain. It is then possible to extract topography from a single orbit of Magellan SAR data. While this approach has its limitations it demonstrates that InSAR analysis is possible at Venus using an S-band SAR.

[38] The question as to whether landsliding is currently occurring on Venus remains open and will best be answered by an InSAR analysis. We propose that a future SAR missions should have a circular orbit resulting in control of the spacecraft, improved data acquisition and processing over Magellan. The SAR should be single or dual frequency (S and L band or L and P band). Variable incidence angles (20° to 50°) should be possible to optimize imaging conditions in areas of steep terrain. The Magellan image resolution was 75m/pixel which was good enough for landslide identification but the details would best be resolved in <5 m/pixel data. The repeat-pass cycle will be dictated by the rotation rate of Venus but 7 to 28 days would be ideal. The derived SAR images could then be used to generate a DEM to be used in differential InSAR analysis.

[39] In conclusion, our study has examined the orbital and imaging parameters required to obtain SAR data suitable for differential InSAR analysis to be successful. Change maps derived from such analysis need to be calibrated with data from ground observations and in situ instruments to be validated. In the case of planetary missions, this requires surface instruments to be designed and deployed, or, for any InSAR results to be calibrated using data from terrestrial landslides that are similar in style. The ability to derive change maps over landslide areas that show displacement is occurring, its extent, and the amount relative to a unit of time from which a rate can be calculated, offers the exciting prospect of being able to answer not only the question as to whether slope deformation is occurring on bodies such as Mars and Venus but also at what rate.

[40] Future work should focus on relating the InSAR maps with subsurface measurements of deformation to gain greater understanding of the relationship between surface deformation and processes occurring in the basal deformation region as well as in the landslide mass itself.

[41] **Acknowledgments.** The authors thank two anonymous reviewers for their comments. We would like to thank Denys Brunnsden and Geoff Davis for discussions regarding Black Ven and for access to the instrument records. This work was funded by the NASA SENH (NAG5-12199) and MDAP program (NAG5-12271).

## References

Adams, J. (2001), Comparing the accuracies of photogrammetry and LIDAR, Thompson Symposium, Rem. Sens. Photo. Soc., Nottingham, UK.

Bray, M. J., D. J. Carter, and J. M. Hooke (1991), Coastal sediment transport study (5 vols.), report to SCOPAC, Dep. of Geogr., Univ. of Portsmouth, Portsmouth, U. K.

Brunnsden, D. (2002), Geomorphological roulette for engineers and planners: some insights into an old game, *Q. J. Eng. Geol. Hydrogeol.*, 35, 101–142.

Brunnsden, D., and J. H. Chandler (1996), Development of an episodic landform change model based upon the Black Ven landslide, 1946–1995, in *Advances in Hillslope Processes*, edited by S. Brooks and M. Anderson, pp. 869–898, John Wiley, Hoboken, N. J.

Brunnsden, D., and D. K. C. Jones (1972), The morphology of degraded landslide slopes in S. W. Dorset, *Q. J. Eng. Geol.*, 5(3), 205–222.

Brunnsden, D., J. C. Doornkamp, P. G. Fookes, D. K. C. Jones, and J. M. H. Kelly (1975), Large scale geomorphological mapping and highway engineering design, *Q. J. Eng. Geol.*, 8, 227–353.

Bulmer, M. H. (1994), Small volcanoes in the plains of Venus; with particular reference to the evolution of domes, Ph.D. thesis, 430 pp., Univ. of London, London.

Bulmer, M. H. (1997), Comparisons between mass movements on Venus associated with modified domes and those from escarpments, *Lunar Planet. Sci.*, XXVIII, part 1, 177–178.

Bulmer, M. H., and J. E. Guest (1996), Modified volcanic domes and associated debris aprons on Venus, in *Volcano Instability*, edited by W. J. McGuire, A. P. Jones, and J. Neuberger, *Spec. Publ. Geol. Soc. London*, 110, 349–371.

Bulmer, M. H., and J. B. Wilson (1999), Comparison of stellate volcanoes on Earth's seafloor with stellate domes on Venus using side scan sonar and Magellan synthetic aperture radar, *Earth Planet. Sci. Lett.*, 171, 277–287.

Bulmer, M. H., and B. A. Zimmerman (2005), Re-assessing landslide deformation in Ganges Chasma, Mars, *Geophys. Res. Lett.*, 32(6), L06201, doi:10.1029/2004GL020201.

Bulmer, M. H., B. A. Campbell, and J. Byrnes (2001), Field studies and radar remote sensing of silicic lava flows, *Lunar Planet. Sci.*, XXXII, abstract 1850.

Camec, C., D. Massonnet, and C. King (1996), Two examples of the use of SAR interferometry on displacement fields of small spatial extension, *Geophys. Res. Lett.*, 23(24), 3579–3582.

Chandler, J. H., and D. Brunnsden (1995), Steady state behavior of the Black Ven mudslide: the application of archival analytical photogrammetry to studies of landform change, *Earth Surf. Process Landforms*, 20, 255–275.

Conway, B. W. (1974), *The Black Ven Landslip, Charmouth, Dorset: An Example of the Effect of a Secondary Reservoir of Groundwater in an Unstable Area*, Her Majesty's Stn. Off., Norwich, U. K.

Denness, B., B. W. Conway, D. M. McCann, and P. Grainger (1975), Investigation of a coastal landslip at Charmouth, Dorset, *J. Eng. Geol. Hydrogeol.*, 8(2), 119–140.

Elachi, C., L. E. Roth, and G. G. Schaber (1984), Spaceborne radar subsurface imaging in hyperarid regions, *IEEE Trans. Geosci. Rem. Sens.*, 22, 383–388.

Ferretti, A., C. Prati, and F. Rocca (2000), Non-linear subsidence rate estimation using permanent scatterers in differential SAR interferometry, *IEEE Trans. Geosci. Remote Sens.*, 38, 2202–2212.

Ferretti, A., C. Prati, and F. Rocca (2001), Permanent scatterers in SAR interferometry, *IEEE Trans. Geosci. Remote Sens.*, 39(1), 8–20.

Ferretti, A., A. Prati, F. Rocca, N. Casagli, P. Farina, and B. Young (2005), Permanent scatterers technology: A powerful state of the art tool for historic and future monitoring of landslides and other terrain instability phenomena, in *Landslide Risk Management: Proceedings of the International Conference on Landslide Risk Management, Vancouver* [CD-ROM], edited by O. Hungr et al., A. A. Balkema, Brookfield, Vt.

Ford, J. P., R. G. Blom, J. A. Crisp, C. Elachi, T. G. Farr, R. S. Saunders, E. E. Theilig, S. D. Wall, and S. B. Yewell (1989), Spaceborne radar observations. A guide to Magellan radar image analysis, *JPL Publ.* 89-41, 126 pp., NASA Jet Propul. Lab., Pasadena, Calif.

Fort, D. S., A. R. Clark, D. T. Savage, and G. M. Davis (2000), Instrumentation and monitoring of the coastal landslides at Lyme Regis Dorset, paper presented at 8th International Symposium on Landslides, Geoenviron. Res. Cent., Cardiff.

Hanssen, R. F. (2001), *Radar Interferometry*, 308 pp., Springer, New York.

Johnson, W. T. K., and A. T. Edgerton (1985), Venus Radar Mapper (VRM): Multimode radar system design, *SPIE Instrum. Opt. Remote Sens. Space*, 589, 158–164.

Lee, H., and J. V. Morgan (2002), Extracting topography of Venus from single orbit Magellan SAR data by using sub-aperture interferometry, *Lunar Planet. Sci.*, 33, abstract 1558.

Luchitta, B. K. (1978), A large landslide on Mars, *Geol. Soc. Am. Bull.*, 89, 1601–1609.

Luchitta, B. K. (1979), Landslides in the Valles Marineris, Mars, *J. Geophys. Res.*, 84, 8097–8113.

Luchitta, B. K. (1987), Valles Marineris, Mars: Wet debris flows and ground ice, *Icarus*, 72, 411–429.

Malin, M. C. (1992), Mass movements on Venus: Preliminary results from Magellan Cycle 1 observations, *J. Geophys. Res.*, 16,337–16,352.

Malin, M. C., et al. (1998), Early views of the Martian surface from the Mars Orbiter Camera of Mars Global Surveyor, *Science*, 279, 1681–1685.

Massonnet, D., and K. L. Feigl (1998), Radar interferometry and its application to changes in the Earth's surface, *Rev. Geophys.*, 36(4), 441–500.

Massonnet, D., M. Rossi, C. Carmona, F. Adragna, G. Peltzer, K. Feigl, and T. Rabaute (1993), The displacement field of the Landers earthquake mapped by radar interferometry, *Nature*, 364, 138–142.

- McEwen, A. S. (1989), Mobility of large rock avalanches: Evidence from Valles Marineris, Mars, *Geology*, 17, 1111–1114.
- Moore, R., and D. Brunsten (1996), Physico-chemical effects on the behaviour of a coastal mudslide, *Geotechnique*, 46(2), 259–278.
- Murphy, W., and R. J. Inkpen (1996), Identifying landslide activity using airborne remote sensing data, *GSA Abstr. Programs*, 28, 28–31.
- Paillou, P., T. W. Thompson, J. J. Plaut, P. A. Rosen, S. Hensley, C. Elachi, D. Massonnet, and J. Achache (2001), MEEM: An orbital synthetic aperture radar for Mars Exploration, paper presented at Conference on the Geophysical Detection of Subsurface Water on Mars, Lunar and Planet. Inst., Houston, Tex.
- Petley, D. N. (1996), The mechanics and landforms of deep-seated landslides, in *Advances in Hillslope Processes*, edited by S. Brooks and M. Anderson, pp. 823–835, John Wiley, Hoboken, N. J.
- Petley, D. N., and R. J. Allison (1997), The mechanics of deep-seated landslides, *Earth Surf. Processes Landforms*, 22, 747–758.
- Petley, D., M. H. Bulmer, and W. Murphy (2002), Patterns of movement in rotational and translational landslides, *Geology*, 30(8), 719–722.
- Petley, D. N., T. Higushi, D. J. Petley, M. H. Bulmer, and J. Carey (2005), The development of landslides in progressive materials, *Geology*, 33(3), 201–204.
- Raucoules, D., C. Carnec, M. Cruchet, C. Delacourt, D. Feurer, and S. Le Moelic (2004), Identification of landslides in La Reunion island with JERS-1 and RADARSAT-1 interferometry, in *FRINGE 2003 Workshop*, Eur. Space Agency Spec. Publ., ESA SP-550.
- Saunders, R. S., et al. (1992), Magellan mission summary, *J. Geophys. Res.*, 97, 13,067–13,090.
- Shaller, P. J. (1991), Analysis and implications of large Martian and terrestrial landslides, Ph.D. thesis, 586 pp., Calif. Inst. of Technol., Pasadena.
- Singhroy, V. (2004), Remote sensing for landslide assessment, in *Landslides Hazard and Risk*, edited by G. Anderson and M. Crozier, pp. 469–492, John Wiley, Hoboken, N. J.
- Singhroy, V., and K. Molch (2004), Characterizing and monitoring rock-slides from SAR techniques, *Adv. Space Res.*, 33(3), 290–295.
- Singhroy, V., and R. Saint-Jean (1999), Effects of relief on the selection of RADARSAT-1 incidence angle for geological applications, *Can. J. Remote Sens.*, 25(3), 211–217.
- Singhroy, V., K. E. Mattar, and A. L. Gray (1998), Landslide characterisation in Canada using interferometric SAR and combined SAR and TM images, *Adv. Space Res.*, 21(3), 465–476.
- Singhroy, V., N. Glenn, D. Bannert, M. H. Bulmer, H. Ohkura, H. Rott, J. Wasowski, C. J. van Westen, and L. Zan (2003), Landslide hazards report, in *The Use of Earth Observing Satellites for Hazard Support: Assessment and Scenarios*, Comm. On Earth Obs. Satellites, NOAA.
- Smith, D. E., et al. (1998), Topography of the northern hemisphere of Mars from the Mars Orbiter Laser Altimeter, *Science*, 279, 1686–1692.
- Squarzoni, C., C. Delacourt, and P. Allemand (2003), Nine years of spatial and temporal evolution of the La Valette landslide observed by SAR interferometry, *Eng. Geol.*, 68(1–2), 53–66.
- Team X (2000), *Mars SAR*, Mars Environ. Evol. Mission, Jet Propul. Lab., Pasadena, Calif.
- Terzaghi, K. (1950), Mechanisms of landslides, in *Application of Geology to Engineering Practice: Berkeley Volume*, pp. 83–123, Geol. Soc. of Am., Boulder, Colo.
- Vachon, P. W., D. Geudtner, A. L. Gray, and R. Touzi (1995), ERS-1 synthetic aperture radar repeat-pass interferometry studies: Implications for RADARSAT, *Can. J. Remote Sens.*, 21, 441–454.

---

M. H. Bulmer, Landslide Observatory, Joint Center for Earth Systems Technology, University of Maryland Baltimore County, Baltimore, MD 21250, USA. (mbulmer@jcet.umbc.edu)

F. Mantovani, Dipartimento di Scienze della Terra, Università di Ferrara, I-44100 Ferrara, Italy.

W. Murphy, School of Earth Sciences, University of Leeds, Leeds LS2 9JT, UK.

D. N. Petley, International Landslide Centre, University of Durham, Durham DH1 3LE, UK.